ELSEVIER

Mathematical Biosciences 162 (1999) 33–51

Mathematical Biosciences
an international journal

www.elsevier.com/locate/mathbio

# Dynamics of influenza A drift: the linear three-strain model

Juan Lin [a,*], Viggo Andreasen [b], Simon A. Levin [c]

[a] *Department of Physics, Washington College, Chestertown, MD 21620, USA*
[b] *Department of Mathematics and Physics, Roskilde University, DK-4000, Roskilde, Denmark*
[c] *Department of Ecology and Evolutionary Biology, Eno Hall, Princeton University, Princeton, NJ 08544, USA*

Received 2 April 1998; received in revised form 12 July 1999; accepted 19 August 1999

**Abstract**

We analyze an epidemiological model consisting of a linear chain of three cocirculating influenza A strains that provide hosts exposed to a given strain with partial immune cross-protection against other strains. In the extreme case where infection with the middle strain prevents further infections from the other two strains, we reduce the model to a six-dimensional kernel capable of showing self-sustaining oscillations at relatively high levels of cross-protection. Dimensional reduction has been accomplished by a transformation of variables that preserves the eigenvalue responsible for the transition from damped oscillations to limit cycle solutions. 

*Keywords:* Influenza drift; Multiple strains; Cross-immunity

## 1. Introduction

The simultaneous circulation of several antigenic variants of the same pathogen can give rise to complex dynamics, including sustained oscillations and chaos in disease prevalence when the pathogen confers sufficiently strong

* Corresponding author.
*E-mail address:* juan.lin@washcoll.edu (J. Lin)

0025-5564/99/$ - see front matter 
PII: S0025-5564(99)00042-5

cross-protection against related strains to recovering hosts [1]. Previous efforts to illustrate how periodic dynamics can be sustained in disease systems have necessarily invoked a complex of factors; in this paper we demonstrate that in a system with three interacting strains, herd-immunity alone can support sustained oscillations. The simplest such case is the 'linear three-strain model', in which one of the strains is of an intermediate type in the sense that it confers partial cross-protection to the two other strains while these two strains induce no reciprocal cross-reaction.

The cocirculation of cross-reacting pathogen types is of interest from both ecological and evolutionary viewpoints. In a few diseases, such as influenza A and canine pavovirus, new antigenic variants arise continuously thus affecting significantly the epidemiology of the disease. Other pathogens display antigenic variation that seems to play no role in the epidemiology of these diseases [2], though the evolutionary forces that maintain this variation remain important to study. Our focus in this paper will be on the influenza A virus, which has been particularly well studied.

Influenza A is an RNA virus of the *Orthomyxoviridae* family [3]. Its persistence in many vertebrate species appears to be linked to its high degree of genetic plasticity [4,5]. Two processes cause the rapid evolution of the glycoprotein molecules, hemagglutinin (HA) and neuraminidase (NA), on the surface of the virus: antigenic drift and genetic shift [6,7]. In antigenic drift, point mutations in HA and NA gradually change the aminoacid composition of antigenic sites. These mutants or strains are responsible for annual or biennial epidemics affecting tens of millions of people worldwide. In genetic shift, gene reassortment in the negatively charged segments of the nuclear RNA gives rise to a new virus subtype with a different set of antibody binding sites (epitopes) in the HA and NA molecules [8]. This virus shift is responsible for the pandemics of 1918 (Spanish flu, $H_1N_1$ subtype), 1957 (Asian flu, $H_2N_2$ subtype) and 1968 (Hong Kong flu, $H_3N_2$ subtype). Although before the Russian flu of 1977 only one subtype was present at any one time, since then both subtypes $H_1N_1$ and $H_3N_2$ have been cocirculating worldwide [9,10]. There is still no clear understanding of why this change has occurred [11–13].

Cross-immunity between different subtypes of influenza A is weak or difficult to detect [14–17]. This is not so with drift variants of the same subtype. Functionally related strains show partial cross-reaction to the antibodies produced in the host against a previous virus strain [18–20]. The degree of cross-reaction between two strains can be identified serologically from hemagglutination inhibition with antibodies reacting fully with one of the strains [21]. Partially cross-reacting strains are functionally related, and zero cross-reactivity means no cross-protection with the antibodies produced in the host against a previous virus strain.

Theoretical studies of cross-immunity in disease transmission dynamics are relatively few. By keeping track of hosts infected with each single strain, one is

naturally led to consider extensions of the well-known continuous-time SIR models to describe the outcomes of selection on a group of strains [22,23]. Models incorporating partial cross-immunity between two strains have been shown to maintain sustained oscillations when age-specific mortalities are included [24,25], or when disease is transmitted by a vector [26]. These oscillations become weakly damped without some sort of delay [27,28].

In a previous paper [29] we analyzed an epidemiological model of influenza A drift that included life-long partial cross-protection among neighboring strains. When strains are placed on a one-dimensional lattice with periodic boundary conditions and partial cross-protection to nearest neighbors, it is found that at relatively high levels of cross-protection sustained oscillations are possible only if the number of cocirculating strains exceeds three. In this paper we show that it is also possible to have a Hopf bifurcation to a periodic solution even when only three strains, in a linear chain configuration, are cocirculating. Therefore, the presence of oscillations does not rely on the cyclic nature of the immunity structure as in [29], but may occur when immunity is organized linearly, mimicking the immunity structure that arises under antigenic drift.

It has recently been shown that the evolutionary tree of the hemagglutinin gene has the shape of a cactus tree with the main trunk of surviving genes evolving significantly faster than the short lateral branches of non-surviving genes [30]. To some this is a sign of positive Darwinian evolution [31,32], while others take a more cautionary view [33]. In this paper we study the dynamics of virus drift for the surviving lineage when the total virus population is divided in subgroups with varying degrees of cross-protection among strains.

In the first part we outline the linear three-strain model, using an index set notation to describe population subgroups with a particular history of infection. In the second part we study a submodel that exhibits sustained oscillations. This submodel has the property that individuals infected with the middle strain are immune to further infections by the other two symmetrical strains. By taking advantage of the remaining symmetry imposed on this submodel we further reduce it to a six-dimensional system. This is so far the simplest system we have been able to find that has self-sustaining oscillations.

## 2. The linear three strain model

The easiest way to convey the structure of the model is to start with an index set notation as described in [29]. Let $K = \{1, 2, 3\}$ be the set of three strains and $J$ be a subset of $K$. Define $S_J$ as the number of susceptible hosts who have previously been infected with strains in $J$, $S_0$ as the completely susceptible class, $I_0^i$ as the number of first time infectives carrying strain $i$, and $I_J^i$ as the number of infectives currently carrying strain $i$ but previously infected with strains in $J$.

We impose $i \notin J$ to account for life-long immunity after a host has been infected with a given strain. The dynamics of infection for the completely susceptible and first time infectious classes are given as follows:

$$\dot{S}_0 = b - \mu S_0 - \sum_{i \in K} \Lambda^i S_0,$$
$$\dot{I}_0^i = \Lambda^i S_0 - (\mu + v) I_0^i, \quad i \in K.$$

First time susceptibles are introduced at a constant rate $b$, die at a constant rate $\mu$, and are removed by infected individuals with a force of infection $\Lambda^i = \beta_i \sum_{J \subseteq K \setminus i} I_J^i$. The transmission coefficient $\beta_i$ measures the infectivity of strain $i$, and changes in most cases from strain to strain. The coefficient $v$ is the recovery rate of infectives, which we assume to be the same for all classes. The equations for $S_J$ and $I_J^i$ are

$$\dot{S}_J = \sum_{j \in J} v I_{J \setminus j}^j - \mu S_J - \sum_{i \notin J} \sigma_J^i \Lambda^i S_J \quad \text{for } J \subseteq K,\ J \neq \emptyset,$$
$$\dot{I}_J^i = \sigma_J^i \Lambda^i S_J - (\mu + v) I_J^i \quad \text{for } J \subseteq K \setminus i,\ J \neq \emptyset.$$

The flow into the class $S_J$ consists of all infectives who are recovering from strain $j \in J$ and who are already immune to all other strains in $J$. The notation $J \setminus j$ represents the set $J$ with strain $j$ removed. Cross-immunity reduces the susceptibility of individuals who are immune to the strains in $J$ to infection by strain $i, i \notin J$, by a factor $\sigma_J^i$. In the three-strain model we will study, there are twelve $I$ variables and eight $S$ variables.

The total population $N$ satisfies the equation

$$\dot{N} = b - \mu N.$$

To avoid the complications of an expanding population we impose $b = \mu N^*$, where $N^*$ is the constant total population at equilibrium. This is a relatively good approximation as long as we keep the time scale of observation small compared to the time scale of global population change. Dividing every equation by $N^*$ gives us the evolution of each class as a fraction of $N^*$. We represent these fractions using the same notation as for subgroups.

The model outlined above can be written in non-dimensional form by defining the time scale in units of the global recovery time $(v + \mu)^{-1}$ of infectives. Using the rescaled mortality $e = \mu/(\mu + v)$ and transmission $r_i = \beta_i N^*/(\mu + v)$ coefficients, and evaluating the time derivative in the re-scaled time $t' = (v + \mu)t$, we can rewrite the model as

$$\begin{aligned}
\dot{S}_0 &= e(1 - S_0) - \sum_{i \in K} \Lambda^i S_0, \\
\dot{S}_J &= \sum_{j \in J} (1 - e) I_{J \setminus j}^j - e S_J - \sum_{i \notin J} \sigma_J^i \Lambda^i S_J, \\
\dot{I}_0^i &= \Lambda^i S_0 - I_0^i, \\
\dot{I}_J^i &= \sigma_J^i \Lambda^i S_J - I_J^i,
\end{aligned} \tag{1}$$

where $\Lambda^i = r_i \sum_{J \subseteq K \setminus i} I_J^i$ is the re-scaled force of infection for strain $i$. Because the total population is constant, the fraction of the population that is immune to all strains, $S_K$, can be removed from the set of essential variables. This subclass can be found from Eq. (1) as

$$S_K = \frac{1-e}{e} \sum_{j \in K} I_{K \setminus J}^j.$$

With a large number of potentially distinct coefficients in the model, the analysis of bifurcation regimes becomes difficult. To focus on a 'linear' situation as outlined in the introduction, we assume that strains 1 and 3 confer no reciprocal cross-immunity, i.e., that $\sigma_3^1 = \sigma_1^3 = 1$, that they confer the same immunity to strain 2, $\sigma_1^2 = \sigma_3^2 = \sigma < 1$, and that no additional protection arises from having been exposed to both strains, $\sigma_{13}^2 = \sigma$. To simplify the analysis we assume that strain 2 induces full protection against strains 1 and 3, i.e., $\sigma_2^1 = \sigma_2^3 = \sigma_{12}^3 = \sigma_{23}^1 = 0$. Furthermore, we assume that strains 1 and 3 have the same transmission coefficient, $r_1 = r_3$. These assumptions preserve the symmetry of the model. Fig. 1 depicts a sketch of the model.

The basic transmission constants $r_i$ measure the average number of secondary infections caused by a single infected host in a susceptible population. Experimental values of $r_i$ for propagating influenza A strains range from 2 to 6 [34]. When mortality is independent of age, $\mu$ is the inverse of the life expectancy of an average individual $\approx$ (70 years)$^{-1}$. Therefore, in most cases the

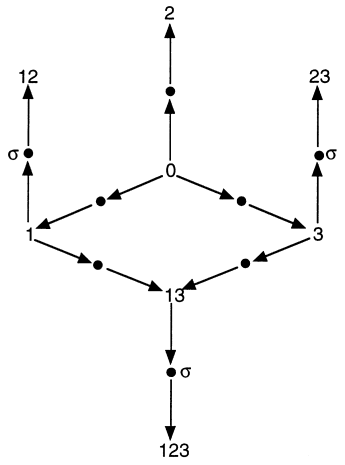


Fig. 1. Dynamics of infection. The numbers between arrows refer to susceptible classes $S_J$. Black dots refer to infectious classes $I_J^i$, $i$ being the index of the new strain appearing at the end of the arrow. There is cross-immunity factor $\sigma$ to infection with strain 2 in hosts previously infected with strains 1, 3 or both, while hosts previously infected with strain 2 are immune to strains 1 and 3.

observed value of $e$ is of the order of 0.0001 when the recovery time $v^{-1}$ ranges from 2 to 6 days.

## 3. Dimensional reduction and steady states

The condition $\sigma_2^i = 0$ implies that individuals previously infected with strain 2 are immune to further infections by strains 1 and 3. A consequence of this restriction is the elimination of the variables $I_2^1, I_2^3, I_{23}^1$ and $I_{12}^3$ from the model since there is no flow into any of these classes. Furthermore, the susceptible subgroups $S_2, S_{12}, S_{23}$ are removable in the following sense. As the arrows in Fig. 1 indicate, they become terminal classes no longer involved in the disease transmission dynamics. The steady state values of the removable $S_J$ can be obtained from the second equation of system (1)

$$S_J = \frac{\sum_{j\in J}(1-e)I_{J\setminus j}^j}{e + \sum_{i\notin J}\sigma_J^i \Lambda^i}.$$

It is easy to verify that the Jacobian matrix for the linearization at any steady state has only negative non-vanishing terms along the diagonal for the four $S$ variables mentioned above. Furthermore, as their steady states do not appear in the remaining equations, their omission will not alter conclusions about stability. Finally, we observe that all $I_J^2$-variables affect the transmission dynamics in the same way and that the flow out of these variables is always into terminal classes. Thus we need only keep track of

$$\Lambda^2 = r_2(I_0^2 + I_1^2 + I_3^2 + I_{13}^2). \tag{2}$$

There are nine equations remaining in the model.

We now take advantage of the significant degree of symmetry between strains 1 and 3 (refer to Fig. 1). Strains 1 and 3 interact only through 'viral interference', i.e., they interact only because simultaneous infections with two strains are impossible. The effect of viral interference is of the order of the duration of infection $O(e)$ and consequently, one strain can prevent the other from invading only if $\Lambda^1 = O(e^2)$ or $\Lambda^3 = O(e^2)$. For details see [22]. This observation suggests that equilibria where only strains 1 or 3 are present will be unstable except near bifurcations where $\Lambda^1 \approx \Lambda^3 \approx 0$. Similarly, the dynamic equations for $\Lambda^1$ and $\Lambda^3$ show that if strains 1 and 3 are both present at equilibrium, they must occur with the same prevalence. In Appendix A we prove this result. Here we neglect such details of viral interference and focus on sums and differences of variables associated with the two strains. Thus, we define a new set of variables,

$$\begin{aligned} S_\pm &= S_1 \pm S_3, \quad I_0^\pm = I_0^1 \pm I_0^3, \\ I_1^\pm &= I_3^1 \pm I_1^3, \quad \Lambda^\pm = r_1(I_0^\pm + I_1^\pm) \end{aligned} \tag{3}$$

while leaving the variables $S_0, S_{13}$ and $\Lambda^2$ unchanged. In these plus–minus variables the system simplifies to

$$\begin{aligned} \dot{S}_0 &= e(1 - S_0) - S_0(\Lambda^+ + \Lambda^2), \\ \dot{S}_\pm &= -eS_\pm + (1-e)I_0^\pm - \tfrac{1}{2}(S_\pm \Lambda^+ - S_\mp \Lambda^-) - \sigma S_\pm \Lambda^2, \\ \dot{S}_{13} &= -eS_{13} + (1-e)I_1^+ - \sigma S_{13}\Lambda^2 \end{aligned} \tag{4a}$$

and

$$\dot{I}_0^\pm = -I_0^\pm + S_0 \Lambda^\pm, \tag{4b}$$

$$\dot{\Lambda}^\pm = -\Lambda^\pm + r_1 S_0 \Lambda^\pm \pm \tfrac{1}{2} r_1 (S_\pm \Lambda^+ - S_\mp \Lambda^-), \tag{4c}$$

$$\dot{\Lambda}^2 = -\Lambda^2 + r_2(S_0 + \sigma S_+ + \sigma S_{13})\Lambda^2, \tag{4d}$$

where $I_1^+$ is determined by the equation $\Lambda^+ = r_1(I_0^+ + I_1^+)$. By symmetry, all minus variables vanish at symmetric steady states and the linearization decomposes the system into two invariant subspaces: a six-dimensional subspace for the plus variables, $S_0$, $S_{13}$, and $\Lambda^2$, and a three-dimensional space for the minus variables. In Appendix A we show that the origin – i.e. $\Lambda^- = 0$, etc. – is always asymptotically stable in the minus subspace. Next, by generalizing the results from the theory of epidemics in structured populations, one can express equilibrium values of the state variables as functions of $\Lambda^+$ and $\Lambda^2$. Equilibria are now determined as the non-negative solutions to the steady state conditions on $\Lambda^+$ and $\Lambda^2$, cf. Eqs. (4c) and (4d). Furthermore, one can show that the stability of the boundary equilibria are determined by the invasion conditions for the strains not present. For details see [29].

There are four types of steady states of Eqs. (4a)–(4d). We proceed to discuss each type separately.

### 3.1. Disease free equilibrium

In this case the total population belongs to the susceptible group $S_0$, and the equilibrium state $O_0$ is given by

$$O_0: \quad S_0 = 1.$$

We check the stability of this state $O_0$ by studying under which conditions any of the strains can invade $S_0$. The appropriate variables to consider are the forces of infection $\Lambda^+ = \Lambda^1 + \Lambda^3$ and $\Lambda^2$. They obey the following equations near the disease free equilibrium,

$$\dot{\Lambda}^+ = \Lambda^+(-1+r_1), \quad \dot{\Lambda}^2 = \Lambda^2(-1+r_2).$$

Thus the state $O_0$ is only stable if both $r_1$ and $r_2$ remain below 1.

### 3.2. Strain 2 alone

Provided $r_2 > 1$, the steady state $O_2$ involving only strain 2 is given as

$$O_2: \quad S_0 = \frac{1}{r_2}, \quad S_2 = \left(1-\frac{1}{r_2}\right)(1-e), \quad I_0^2 = e\left(1-\frac{1}{r_2}\right),$$

while all other variables vanish. To find the stability of $O_2$ to invasion by strains 1 and 3 we observe that since either strain can invade, the most appropriate variable to consider is the force of infection $\Lambda^+$. An equation for $\Lambda^+$ can be found directly from (4c),

$$\dot{\Lambda}^+ = r_1(S_0 + \tfrac{1}{2}S_+)\Lambda^+ - \Lambda^+. \tag{5}$$

When $S_0$ and $S_+$ are evaluated at $O_2$ the previous expression simplifies to

$$\dot{\Lambda}^+ = \left(\frac{r_1}{r_2} - 1\right)\Lambda^+.$$

Therefore, we observe that strains 1 and 3 cannot invade if $r_1 < r_2$; the equilibrium $O_2$ is only stable above the line

$$L_2: \quad r_2 = r_1.$$

### 3.3. Coexistence of strains 1 and 3 alone

A second (symmetric) boundary equilibrium $O_{13}$ is given by

$$O_{13}: \quad S_0 = \frac{1}{2r_1-1} + \mathrm{O}(e), \quad S_+ = \frac{2(r_1-1)}{r_1(2r_1-1)} + \mathrm{O}(e),$$

$$S_{13} = \frac{2(r_1-1)^2}{r_1(2r_1-1)} + \mathrm{O}(e),$$

$$I_0^+ = \frac{2e(r_1-1)}{2r_1-1} + \mathrm{O}(e^2), \quad I_1^+ = \frac{2e(r_1-1)^2}{r_1(2r_1-1)} + \mathrm{O}(e^2), \quad \Lambda^2 = 0.$$

We now analyze the stability of this steady state to invasion by strain 2. The dynamics of strain 2 is determined by (4d) and we find that $O_{13}$ can be invaded only if

$$r_2(S_0 + \sigma S_+ + \sigma S_{13}) > 1,$$

where all variables are evaluated at $O_{13}$. This condition yields the bifurcation curve

$$L_{13}: \quad r_2 = \frac{2r_1 - 1}{1 + 2\sigma(r_1 - 1)}$$

for $e \ll 1$. Only below this boundary curve is the steady state $O_{13}$ stable. The condition for a common area where both stable steady states $O_2$ and $O_{13}$ coexist is given by $dr_2/dr_1 > 1$, or equivalently, by $\sigma < 1/2r_1$ (refer to Fig. 2). The stability of the two-strain steady state for systems equivalent to this one has already been analyzed [22,24,27].

### 3.4. All strains present

We now proceed to discuss the existence and stability of internal equilibria in the case $1/2 - \sigma > 0$. Solving for $S_J$ by using the equilibrium condition in (4a)–(4d) we find

$$1 = r_1(S_0 + \tfrac{1}{2}S_+), \tag{6a}$$

$$1 = r_2(S_0 + \sigma S_+ + \sigma S_{13}), \tag{6b}$$

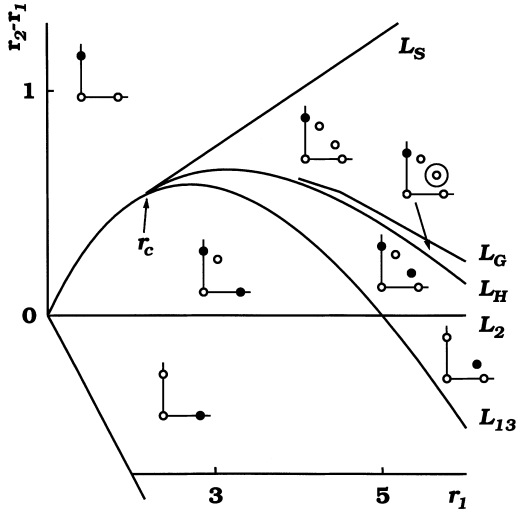


Fig. 2. Bifurcation diagram of model (1) for equilibria that are symmetric in strains 1 and 3. The curves $L_2$, $L_{13}$ and $L_S$ refer to bifurcations at $O_2$, $O_{13}$, and the saddle-node bifurcation discussed in Section 3.4 The phase portraits are 2-D representations of the dynamics of infection where the horizontal axis refer to $A^+$ and the vertical axis to $A^2$. In the phase portraits a filled circle indicates a stable equilibrium while an open circle indicates an unstable equilibrium. The system undergoes a Hopf bifurcation on the curve $L_H$. On curve $L_G$ the limit cycle disappears in a saddle-node bifurcation. The complete bifurcation diagram has regions with negative equilibrium states. Our diagram shows only the biologically meaningful equilibria. The continuation of the line $L_S$ for $r_1 < r_c$ is not shown as in this regime $A^2$ is negative. Parameter values used in the diagram: $e = 10^{-2}$ and $\sigma = 0.1$.

where the $S_J$s are functions of $\Lambda^+$ and $\Lambda^2$. These two equations can be reduced to a quadratic equation in say $\Lambda^2$. It is not hard to see that this equation has two roots only when $r_2$ lies below the line

$$L_S: \quad r_2 = \frac{r_1}{1/2 + \sqrt{\sigma(1-\sigma)}}. \tag{7}$$

The two bifurcation curves $L_S$ and $L_{13}$ meet tangentially at $r_1 = r_c$ where

$$r_c = \frac{1}{2} + \frac{1}{2}\sqrt{\frac{1}{\sigma} - 1}.$$

Fig. 2 shows the locations of all non-trivial equilibria and in Appendix B we provide details of these calculations. The small size of the parameter region in which periodic solutions occur, seems most likely to be related to the small number of strains (there are no sustained oscillations in the two-strain model)

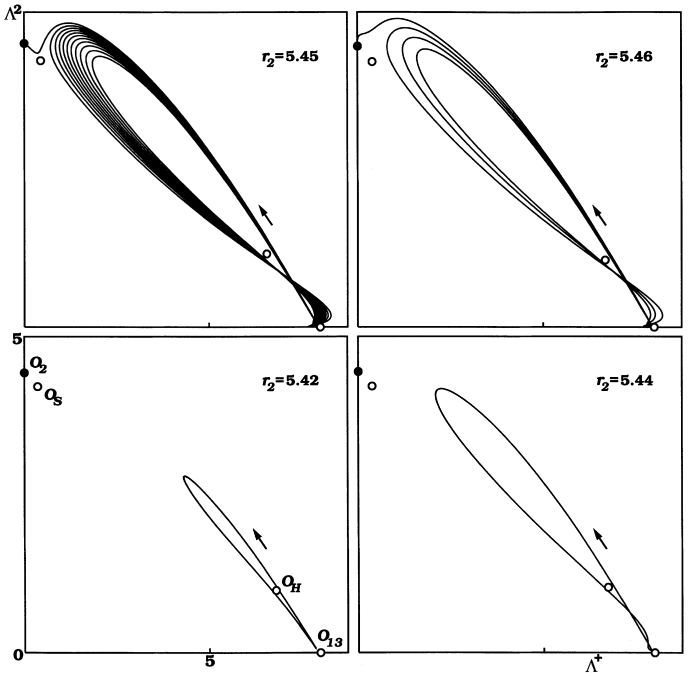


Fig. 3. Phase portraits of the 20-dimensional model (1) projected on the rescaled forces of infection $(\Lambda^+, \Lambda^2)$. The open and closed circles represent unstable and stable equilibria, respectively. At $r_1 = 5$ the equilibrium $O_H$ undergoes a Hopf bifurcation at $r_2 \approx 5.41$ creating a stable limit cycle. At $r_2 \approx 5.42$ the limit cycle is fully developed and at $r_2 \approx 5.45$–$5.46$ we observe the disappearance of limit cycle when it meets the stable manifold of the internal equilibrium $O_S$ tangentially. Parameter values used in the diagram: $e = 0.01$, $\sigma = 0.1$ and $r_1 = 5$.

and to the constraints imposed by the specific symmetric interactions in the model. The limit cycle region expands considerably when four or more strains are configured in a closed chain with periodic boundary conditions [29].

Numerical computation of the spectrum of the linearization, via the Q-R algorithm [35], shows that the branch of roots $O_S$ that changes sign at the $O_2$ boundary curve ($r_1 = r_2$) is always unstable. The other branch of roots $O_H$ is stable near the $O_{13}$ boundary curve, but as $r_2$ is increased beyond the curve $L_{13}$ it undergoes a Hopf bifurcation to a stable limit cycle along a curve $L_H$. Numerical solutions of the dynamical model also suggest that the limit cycle disappears in a global bifurcation that seems to involve a saddle connection bifurcation at $O_S$; see Fig. 3 for a numerical solution of the transition in the

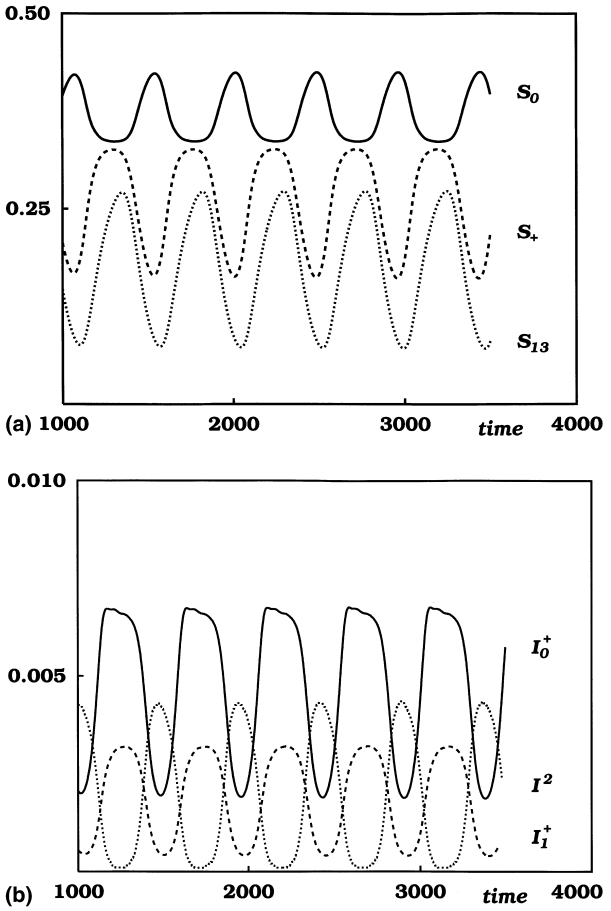


Fig. 4. Oscillations in the six-dimensional kernel consisting of $S_0, S_+, S_{13}, I_0^+, I_1^+$ and $I^2 = \Lambda^2/r_2$. Parameter values used in the simulation are $r_1 = r_2 = 2$ and $\sigma = 0.3$.

reduced space $(\Lambda^+, \Lambda^2)$. The dynamical picture described above has been found to be consistent with the bifurcation diagram obtained from a standard continuation-bifurcation software [36]. Additional details of a similar computation can be found in [29].

Although the separation of the dynamics into subspaces associated with the minus- and plus-variables holds only in the linearization of endemic equilibria, we have found numerically that in the limit, the minus sign variables always vanish. The essential dynamics of the model are therefore determined by the six-dimensional kernel associated with the plus-variables. The (1, 3)-symmetry, however, appears to be particular to the present model. Ferguson et al. [37] reports that such symmetry may break down in multi-strain models with similar structure.

A numerical solution of the 6-D subsystem is shown in Fig. 4. The simulations have been done with $e = 0.01$ and $r_1 = r_2 = 2$ to demonstrate the size and phase of oscillations. In a more realistic situation we would have $e \approx 0.0001$ for a life expectancy of $\approx$70 years and $v \approx 120$/year for a recovery time of $\approx$3 days. This latter scenario would give us for $\sigma = 0.3$, an oscillation period of $\approx$10,000 time units instead of the $\approx$500 time units shown in Fig. 4. In real time $t = t'/(\mu + v)$, the 10,000 units is equivalent to a period of approximately 80 years. The period decreases roughly by a factor of two if the $r$'s are increased to $r_1 \approx r_2 \approx 5$.

## 4. Discussion

The problem of periodic oscillations in influenza dynamics has long attracted theoretical interest. Previous explanations have relied on aspects of age structure and cross-immunity relations among different strains. Recently, it has been shown that in a non-age-structured population with four circulating strains obeying a cross-immunity structure with strong symmetry properties, sustained oscillations can be maintained [29]. In this paper, we demonstrate that the oscillations can also be sustained with as few as three strains.

A robust feature of complex adaptive systems is that they become self-organized hierarchically into tightly-interacting clusters of elements that in turn interact only weakly with elements in other clusters [38,39]. Influenza is no exception, as strains become organized into quasispecies and subtypes that exhibit strong cross-reactivity within these clusters, and weak cross-reactivity among them [1,29]. The investigations of this paper, focusing on intermediate levels of cross-reactivity, may be viewed as most appropriate for describing the interactions among clusters of strains that represent a level between the strain and the subtype – in the simplest case, a subtype may be viewed as being organized say into three interacting clusters of strains. The investigations of this paper show that, generically, one might expect to see the period waxing and

waning of these clusters on the order of the life span of humans, 40–80 years. In practice, such fluctuations might lead to fade-outs of strain clusters at local levels, but the central point is that the loss of herd immunity on these scales determine the time scale for reemergence due to shift. With this interpretation, the predictions of the model are consistent with observed time scales of re-emergence, although alternative explanations are certainly possible.

The model where the intermediate strain induces complete immunity is not the only configuration in the linear chain that admits sustained oscillations. A second model, this time characterized by assuming that individuals become immune to infections by the middle strain once they have been infected by one of the two symmetrical strains, can also display limit cycle oscillations. Yet the minimal system capable of describing this behavior appears to be nine-dimensional.

An essential ingredient to produce sustained oscillations seems to be the presence of multiple steady states for some combination of parameter values. This structure differs from that of interacting viruses with complete cross-immunity following SIR-type dynamics. Here the stability of the boundary equilibria is linked so that no more than one equilibrium is stable for any set of parameter values, thus leading to a 'competitive exclusion principle' [40]. Including partial cross-immunity in the dynamics of virus propagation may therefore be of central importance when studying virus polymorphism.

The bifurcation structure in the present model is quite similar to that of [29]. In particular, the presence of sustained oscillations that disappear through a global bifurcation is a common feature. The challenge remains to elucidate further this bifurcation, especially the complicated transition that takes place where the bifurcation curves meet tangentially in Fig. 2. The diagram in Fig. 2 seems to suggest the presence of a co-dimension two bifurcation involving a double zero-eigenvalue, but the size of the model in combination with the small parameter $e$ has excluded a detailed numerical verification.

Although the linear model has the same basic patterns as does the four-strain model of [29], the analysis is different. Clearly, the formal analysis of such a high-dimensional system remains difficult, but examination of the extreme case $\sigma_2^i = 0$ illustrates the main aspects of cross-immunity in disease transmission. Focusing on the case $\sigma_2^i = 0$, corresponding to a cross-immunity structure where the intermediate strain 2 confers complete immunity to the other two strains, we were able to reduce the model to a nine-dimensional system. By 'folding' subclasses into plus–minus variables we managed to identify a six-dimensional subspace in which sustained oscillations occur. The basic idea of this approach may be applied to other systems of strains conferring cross-immunity. For example, in the four-strain system of [29] one can reduce the original 48-dimensional system to one with 20 variables. In doing so we must ensure consistency if the index structure in $I_J^i$ with those in $S_J$. In the folded model the new variables are,

$$\{S_0, S_{1+}, S_{2+}, S_{13}, S_{24}, S_{++}, S_{123+}, S_{124+}\},$$

and the complementary set of 12 infectious groups. We define,

$$S_{1+} = S_1 + S_3, \quad S_{2+} = S_2 + S_4, \quad S_{++} = \sum_{i,j} S_{ij} - S_{13} - S_{24},$$

$$S_{123+} = S_{123} + S_{134} \quad \text{and} \quad S_{124+} = S_{124} + S_{142}.$$

The remaining variables are easy to write. The classes $S_1(S_2)$ and $S_3(S_4)$ have been folded, but $S_{13}(S_{24})$ are left undisturbed. Failure to do so will eliminate the strong interaction 1->3($\sigma = 1$) and the system will not be able to exhibit a Hopf bifurcation. It appears, at least numerically, that the eigenvalue spectrum of the 20 variable system is a subset of the spectrum of the full model. Yet this reduction does not yield a sufficiently simple model that will permit us to study the parameter dependence of oscillations past the supercritical Hopf bifurcation. The same comments apply to all other higher order models.

The model developed in this paper offers a static view of mutation. The initial space of strains once defined is closed to further changes. It does not allow for drift mutation to generate new strains to displace old ones [41]. A way out of this constraint is to assume a one-dimensional continuum of strains where infection with a given strain $x$ (characterized by its position on the line) confers immunity to all other strains before $x$. Drift mutation, the driving process to avoid host immunity, is incorporated into the model as a diffusion process. Preliminary results indicate that such a continuous view of mutation allows for the existence of stable travelling waves [42] moving at a constant velocity. Ideally, one would like to combine the stochasticity of drift mutation with the dynamics of a group of strains, viewed as a quasispecies [43], to understand how cross-immunity shapes the coevolution of host and virus.

## Acknowledgements

This work has been supported in part by a NATO Collaborative Research Grant 940704.

## Appendix A. Excluding endemic (1, 3)-asymmetric equilibria

We first show that any equilibrium where strains 1 and 3 are both present must be symmetric in the two strains. To see this, first observe that the equilibrium conditions for $A^i$, $i = 1, 3$ yield

$$0 = \Lambda^i(r_1(S_0 + S_j) - 1), \quad i = 1, 3, \ \ j = 3, 1.$$

Since by assumption $\Lambda^i \neq 0$, this gives $S_1 = S_3$, or $S_- = 0$.

The equation for $\dot{S}_- = 0$ now simplifies to

$$0 = (1 - e)I_0^- + \tfrac{1}{2}S_+\Lambda^- = ((1 - e)S_0 + \tfrac{1}{2}S_+)\Lambda^-,$$

where we have used the equilibrium condition $I_0^- = S_0\Lambda^-$. Therefore, we conclude that $\Lambda^- = 0$.

### *A.1. Stability of the minus system* $\{S_-, I_0^-, \Lambda^-\}$

The minus system obtained from Eqs. (4a)–(4c) is a linear system with coefficients dependent on the plus variables evaluated at an interior steady state. To prove the stability of this subspace we analyze the Jacobian matrix

$$M = \begin{pmatrix} -e - \frac{\Lambda^+}{2} - \sigma\Lambda^2 & 1 - e & \frac{S_+}{2} \\ 0 & -1 & S_0 \\ -\frac{r_1\Lambda^+}{2} & 0 & -1 + r_1S_0 + \frac{r_1S_+}{2} \end{pmatrix}.$$

If we define $A = e + \Lambda^+/2 + \sigma\Lambda^2 > 0$ and use Eq. (6a) in the third diagonal term, $M$ simplifies to

$$M = \begin{pmatrix} -A & 1 - e & \frac{S_+}{2} \\ 0 & -1 & S_0 \\ -\frac{r_1\Lambda^+}{2} & 0 & 0 \end{pmatrix}.$$

The characteristic equation for $M$ has the form

$$P(\Lambda) = \Lambda^3 - \mathrm{Tr}(M)\Lambda^2 + a\Lambda - \det(M)$$

with coefficients

$$\begin{aligned} \mathrm{Tr}(M) &= -A - 1 < 0 \\ a &= A + r_1S_+\frac{\Lambda^+}{4} > 0 \\ \det(M) &= -\tfrac{1}{2}r_1\Lambda^+(S_0(1 - e) + \tfrac{1}{2}S_+) \\ &= -\tfrac{1}{4}r_1S_+(2A + \Lambda^+) < 0, \end{aligned}$$

since according to (4a) the steady state value of $S_+$ is

$$S_+ = \frac{(1 - e)I_0^+}{e + \Lambda^+/2 + \sigma\Lambda^2} = \frac{(1 - e)S_0\Lambda^+}{A}.$$

The Routh–Hurwitz criteria for all eigenvalues of $M$ to have negative real parts require that

$$\mathrm{Tr}(M) < 0, \quad \det(M) < 0, \quad \det(M) - \mathrm{Tr}(M)a > 0.$$

We need only show that the last condition is satisfied. A simple calculation reveals that

$$\begin{aligned}\det(M) - \mathrm{Tr}(M)a &= A(A + 1 + \tfrac{1}{4}r_1 S_+ \Lambda^+ - \tfrac{1}{2}r_1 S_+) \\ &= A(A + r_1 S_0 + \tfrac{1}{4}r_1 S_+ \Lambda^+) > 0,\end{aligned}$$

where we have used the equilibrium condition (6a) in the last line.

## Appendix B. Boundary curve for symmetric internal equilibria

The equilibrium values for the susceptible and infectious classes can be found through (4a)–(4c),

$$\begin{aligned}&I_0^+ = S_0 \Lambda^+, \quad I_1^+ = \frac{1}{2} S_+ \Lambda^+, \quad S_0 = \frac{e}{e + \Lambda^+ + \Lambda^2}, \\ &S_+ = \frac{(1-e)\Lambda^+ S_0}{e + \frac{1}{2}\Lambda^+ + \sigma\Lambda^2}, \quad S_{13} = \frac{(1-e)\Lambda^+ S_+}{2(e + \sigma\Lambda^2)}.\end{aligned} \tag{B.1}$$

To lowest order in $e$ we approximate $1 - e \approx 1$ in (B.1) and scale $\Lambda^+ = ex$ and $\Lambda^2 = ey$. Next, these values are substituted into the equilibrium Eqs. (6a) and (6b) giving

$$\begin{aligned}&(1 + x + y)(1 + \tfrac{x}{2} + \sigma y) = r_1(1 + x + \sigma y) \\ &(1 + \sigma y)(1 + x + y) = r_2(1 + \sigma x + \sigma y).\end{aligned} \tag{B.2}$$

From the second equation of (B.2) we solve for $x$

$$x = \frac{(1 + \sigma y)(1 - r_2 + y)}{-1 + \sigma r_2 - \sigma y}$$

and substitute this expression into the first equation. In the variable $u = r_2 - y$ we find a quadratic equation

$$r_1 \sigma u^2 + ((\tfrac{1}{2} - \sigma)r_2 - r_1)u + \tfrac{1}{2}r_2 = 0,$$

which has two positive real roots for

$$r_1 > r_2(\tfrac{1}{2} + \sqrt{\sigma(1-\sigma)}) \quad \text{and} \quad r_1 > r_c, \tag{B.3}$$

while for $r_1 < r_c$, $y$ is negative.

Our computations so far show that below the saddle-node bifurcation line $L_S$ as defined in Eq. (7), there exists two branches of $(\Lambda^+, \Lambda^2)$-equilibrium values. As discussed in the main text, we may identify the equilibria with these values. In this sense, the equilibrium values are given implicitly by the equations

$$F = S_0(\Lambda^+, \Lambda^2) + \frac{1}{2}S_+(\Lambda^+, \Lambda^2) - \frac{1}{r_1} = 0,$$
$$G = S_0(\Lambda^+, \Lambda^2) + \sigma S_+(\Lambda^+, \Lambda^2) + \sigma S_{13}(\Lambda^+, \Lambda^2) - \frac{1}{r_2} = 0. \tag{B.4}$$

To study the bifurcation at $L_2$ on Fig. 2 we treat $r_1$ as the bifurcation parameter (note that increasing $r_1$ corresponds to moving diagonally to the right and down on the figure). At $L_2$ the boundary equilibrium $O_2 : (0, \Lambda^*)$ satisfies $G = 0$ due to the equilibrium condition and $F = 0$ as

$$S_0(\Lambda^+, \Lambda^2) + \frac{1}{2}S_+(\Lambda^+, \Lambda^2) - \frac{1}{r_1} \text{ evaluated at } O_2 \text{ is } \frac{1}{r_2} - \frac{1}{r_1} = 0.$$

Therefore, $(0, \Lambda^*)$ lies on one branch of equilibria and conversely, if the point $(0, \Lambda)$ with $\Lambda > 0$ satisfies $F = G = 0$, then that point lies on $L_2$. We shall refer to this branch as $O_S(r_1) = (\Lambda_S^+, \Lambda_S^2)$, and let $r^*$ denote the value for which $O_S(r^*) = (0, \Lambda^*)$.

Since the boundary equilibrium $O_2$ is independent of $r_1$, we observe through Eq. (5) that $O_2$ changes stability at $r_1 = r^*$ and that it is unstable for $r_1 > r^*$. To see that the internal equilibrium $O_S$ is positive for $r_1 < r^*$, it suffices to show that

$$\left.\frac{\mathrm{d}\Lambda_S^+}{\mathrm{d}r_1}\right|_{(0,\Lambda^*)} < 0. \tag{B.5}$$

The derivative can be determined by implicit differentiation of $F = 0$ and $G = 0$ with respect to $r_1$. If we write these equations as

$$F_1(\Lambda^+, \Lambda^2) = \frac{1}{r_1} \quad \text{and} \quad G_1(\Lambda^+, \Lambda^2) = \frac{1}{r_2},$$

respectively, then elimination of $\mathrm{d}\Lambda_S^2/\mathrm{d}r_1$ from these equations yields

$$\Delta \frac{\mathrm{d}\Lambda_S^+}{\mathrm{d}r_1} = -\frac{\partial G_1}{\partial \Lambda^2}\frac{1}{r_1^2},$$

where

$$\Delta = \frac{\partial F_1}{\partial \Lambda^+}\frac{\partial G_1}{\partial \Lambda^2} - \frac{\partial F_1}{\partial \Lambda^2}\frac{\partial G_1}{\partial \Lambda^+}.$$

A simple computation shows that $\partial G_1/\partial \Lambda^2 < 0$ for all non-negative $(\Lambda^+, \Lambda^2)$ and that $\Delta < 0$ on $L_2$. Thus we conclude that condition (B.5) holds. Since $\Lambda_S^+(r_1)$ and $\Lambda_S^2(r_1)$ are $C^1$-functions we can in fact conclude that $\Delta(O_S) < 0$ in the region between $L_S$ and $L_2$ and hence that $\Lambda_S^+(r_1)$ is decreasing.

The analysis of the bifurcation at $L_{13}$ can be carried out in a similar way. However, the transversality condition corresponding to (B.5) is slightly more involved. Here it is most convenient to consider $r_2$ as the bifurcation parameter

and divide the discussion into two cases depending on the magnitude of $r_1$. For $r_1 > r_c$, we consider the branch of equilibria for which $O_H(r^{\#}) = (\Lambda^{\#}, 0)$. The transversal crossing of $O_H$ and $O_{13}$ is determined by the value of $d\Lambda_H^2/dr_2$ at $O_{13}$ and we find

$$\Delta \frac{d\Lambda_H^2}{dr_2} = -\frac{\partial F_1}{\partial \Lambda^+} \frac{1}{r_2^2}.$$

A rather long and tedious calculation shows that $\partial F_1/\partial \Lambda^+ < 0$ and $\partial F_1/\partial \Lambda^2 < 0$ on $L_{13}$, whereas $\partial G_1/\partial \Lambda^+ > 0$ and $\partial G_1/\partial \Lambda^2 < 0$ on $L_{13}$. As $\Delta(O_H) > 0$ we conclude that $d\Lambda_H^2/dr_2 > 0$. For $r_1 < r_c$, the computations proceed along the same line except that in this case, $\Delta(O_H) < 0$ so that $d\Lambda_H^2/dr_2 < 0$.

## References

[1] S. Gupta, N. Ferguson, R. Anderson, Chaos persistence and evolution of strain structure in antigenically diverse infectious agents, Science 280 (1998) 912.
[2] E.D. Kilbourne, Host determination of viral evolution: a variable tautology, in: S.S. Morse (Ed.), The evolutionary biology of viruses, Raven, New York, 1994, p. 253.
[3] R.A. Lamb, Genes and proteins of the influenza viruses, in: R.M. Krug, H. Fraenkel-Conrat, R.R. Wagner (Eds.), The influenza viruses, Plenum, New York, 1989, p. 1.
[4] P.E.M. Fine, Applications of mathematical models to the epidemiology of influenza: a critique, in: P. Selby (Ed.), Influenza models, MTP, Lancaster, 1982, p. 15.
[5] S.B. Thacker, The persistence of influenza in human populations, Epidemiol. Rev. 8 (1986) 129.
[6] P. Palese, F.J. Young, Variation of influenza A, B and C viruses, Science 215 (1982) 1468.
[7] R.G. Webster, W.G. Laver, G.M. Air, G.C. Schild, Molecular mechanisms of variation in influenza viruses, Nature 296 (1982) 115.
[8] R.G. Webster, W.J. Bean, O.T. Gorman, T.M. Chambers, Y. Kawaoka, Evolution and ecology of influenza A viruses, Microbiol. Rev. 56 (1992) 152.
[9] C. Stuart-Harris, The epidemiology and prevention of influenza, Amer. Sci. 69 (1981) 166.
[10] F.L. Smith, P. Palese, Variation in influenza virus genes, in: R.M. Krug, H. Fraenkel-Conrat, R.R. Wagner (Eds.), The Influenza Viruses, Plenum, New York, 1989, p. 319.
[11] P.E.M. Fine, Herd immunity: history theory and practice, Epidemiol. Rev. 15 (1993) 265.
[12] A.W. Hampson, Surveillance for pandemic influenza, J. Inf. Dis. 176 (1997) S8.
[13] R.G. Webster, Predictions for future human influenza pandemics, J. Inf. Dis. 176 (1997) S14.
[14] J.P. Fox, Interference phenomena observed in the field, Recent Prog. Microbiol. 8 (1982) 443.
[15] A.L. Frank, L.H. Taber, J.M. Wells, Individuals infected with two sub-types of influenza A virus in the same season, J. Inf. Dis. 147 (1983) 120.
[16] A.S. Monto, J.S. Koopman, I.M. Longini Jr, The Tecumseh study of illness. XII. Influenza infection and disease, 1976–1981. Am. J. Epidemiol. 121 (1985) 811.
[17] E. Ackerman, I.M. Longini Jr, S.K. Seaholm, A.S. Hedin, Simulation of mechanisms of viral interference in influenza, Int. J. Epidemiol. 19 (1990) 444.
[18] R.B. Couch, J.A. Kasel, Immunity to influenza in man, Ann. Rev. Microbiol. 37 (1983) 529.
[19] J.R. Davies, E.A. Grilli, A.J. Smith, Influenza A: infection and reinfection, J. Hyg. Camb. 92 (1984) 125.

[20] J.R. Davies, E.A. Grilli, A.J. Smith, Infection with influenza a H1N1. 2. The effect of past experience on natural challenge, J. Hyg. Camb. 96 (1986) 345.
[21] A.J. Levine, Viruses, W.H. Freeman, New York, 1992, p. 155.
[22] K. Dietz, Epidemiologic interference of virus populations, J. Math. Biol. 8 (1979) 291.
[23] S.A. Levin, D. Pimentel, Selection of intermediate rates of increase in parasite-hosts systems, Am. Nat. 117 (1981) 308.
[24] C. Castillo-Chavez, H.W. Hethcote, V. Andreasen, S.A. Levin, W. Liu, Epidemiological models with age structure, proportionate mixing, and cross-immunity, J. Math. Biol. 27 (1989) 233.
[25] V. Andreasen, Multiple time scales in the dynamics of infectious diseases, in: C. Castillo-Chavez, S.A. Levin, C.A. Shoemaker (Eds.), Mathematical Approaches to Problems in Resource Management and Epidemiology, Springer, Berlin, 1989, p. 142.
[26] S. Gupta, J. Swinton, R.M. Anderson, Theoretical studies of the effects of heterogeneity in the parasite population on the transmission dynamics of malaria, Proc. R. Soc. Lond. B 256 (1994) 231.
[27] W. Liu, S. A. Levin, Influenza and some related mathematical models, in: S.A. Levin, T.G. Hallam, L.J. Gross (Eds.), Applied Mathematical Ecology, Springer, 1989, p. 235.
[28] S.B. Thacker, D.F. Stroup, Persistence of influenza A by continuous close-contact transmission: the effect of non-random mixing, Int. J . Epidemiol. 19 (1990) 1078.
[29] V. Andreasen, J. Lin, S.A. Levin, The dynamics of cocirculating influenza strains conferring partial cross-immunity, J. Math. Biol. 35 (1997) 825.
[30] D.A. Buonagurio, S. Nakada, J.D. Parvin, M. Krystal, P. Palese, W.M. Fitch, Evolution of human influenza A viruses over 50 years: rapid uniform rate of change in NS change, Science 232 (1986) 980.
[31] W.M. Fitch, J.M. Leiter, X. Li, P. Palese, Positive darwinian evolution in human influenza A viruses, Proc. Nat. Acad. Sci. USA 88 (1991) 4270.
[32] S.T. Nichol, J.E. Rowe, W.M. Fitch, Punctuated equilibrium and positive Darwinian evolution in vesicular stomatitis virus, Proc. Nat. Acad. Sci. USA 90 (1993) 10424.
[33] J.H. Gillespie, Episodic evolution of RNA viruses, Proc. Nat. Acad. Sci. USA 90 (1993) 10411.
[34] C.C. Spicer, C.J. Lawrence, Epidemic influenza in Greater London, J. Hyg. Camb. 93 (1984) 105.
[35] W.H. Press, S.A. Teukolsky, W.T. Vetterling, B.P. Flannery, Numerical Recipes in C, second edition, p. 486ff. Cambridge University, New York, 1992.
[36] Y.A. Kuznetsov, V.V. Levitin, CONTENT 1.5. Available via www.cwi.nl/ftp.
[37] N. Ferguson, R. Anderson, S. Gupta, The effect of antibody-dependent enhancement on the transmission dynamics and persistence of multiple-strain pathogens, Proc. Nat. Acad. Sci. USA 96 (1999) 790.
[38] H. Simon, The Science of Artificial Life, MIT, Cambridge, MA, 1969.
[39] S.A. Levin, Fragile Dominion, Perseus Books, Reading, MA, 1999.
[40] H.J. Bremermann, H.R. Thieme, A competitive exclusion principle for pathogen virulence, J. Math. Biol. 27 (1989) 179.
[41] C.M. Pease, An evolutionary epidemiological mechanism with application to type A influenza, Theor. Pop. Biol. 31 (1987) 422.
[42] V. Andreasen, S.A. Levin, J. Lin, A model of influenza A drift evolution, Z. Angew. Math. Mech. 76 (2) (1996) 421.
[43] M. Eigen, J. McCaskill, P. Schuster. The molecular quasispecies, J. Phys. Chem. 92 (1988) 6881.